Kobe University Repository : Kernel

PDF issue: 2025-12-05

UVA- and Visible-Light-Mediated Generation of Carbon Radicals from Organochlorides Using Nonmetal Photocatalyst

Matsubara, Ryosuke ; Yabuta, Tatsushi ; Idros, Ubaidah Md ; Hayashi, Masahiko ; Ema, Fumitoshi ; Kobori, Yasuhiro ; Sakata, Ken

(Citation)
Journal of Organic Chemistry,83(16):9381-9390

(Issue Date)
2018-08-17

(Resource Type)
journal article

(Version)
Accepted Manuscript

(Rights)
This document is the Accepted Manuscript version of a Published Work that appeared in final form in Journal of Organic Chemistry, copyright © American Chemical Society after peer review and technical editing by the publisher. To access the final edited and published work see http://dx.doi.org/10.1021/acs.joc.8b01306

(URL)
https://hdl.handle.net/20.500.14094/90005183

UVA- and visible light-mediated generation of carbon radicals from organochlorides using non-metal photocatalyst

Ryosuke Matsubara,*[,§] Tatsushi Yabuta,[§] Ubaidah Md Idros,[§] Masahiko Hayashi,[§] Fumitoshi Ema,[§] Yasuhiro Kobori,[§] Ken Sakata[¶]

[§] Department of Chemistry, Graduate School of Science, Kobe University, Nada, Kobe 657-8501, Japan

[¶] Faculty of Pharmaceutical Sciences, Toho University, Miyama, Funabashi, Chiba 274-8510, Japan

ABSTRACT: Carbon radicals are reactive species useful in various organic transformations. The C–X bond cleavage of organohalides by photo-irradiation is a common method to generate carbon radicals in a controlled fashion. Despite the recent significant advance in the photocatalytic transformation, the use of organochloride substrates is still a formidable challenge due to the low reduction potential and the high dissociation energy of the C–Cl bond. In this report, we address these issues by using a non-metal organic molecule with a relatively simple structure as a photocatalyst. In this catalyst (bis(dimethylamino)carbazole), the amino groups increase both the HOMO and LUMO energy levels, especially in the former. As a result, compared to the parent molecule, the new catalyst shows experimentally red-shifted absorption in the visible region and forms an excited state with better reducing capability. This photocatalyst was used in the reduction of unactivated aryl chlorides and alkyl chlorides in the presence of hydrogen atom donor at room temperature. The catalytic system can also be applied to the coupling of aryl chlorides with electron-rich arene and heteroarenes to affect the C–C bond forming reactions. Our mechanistic study results support the assumption that carbon radicals are formed from the organochlorides via a single-electron transfer step.

INTRODUCTION

Carbon radicals are short-lived reactive species that can participate in the formation and cleavage of various bonds. Therefore, their formation and utilization in a controlled manner have been an important research topic in organic chemistry.[1] Since carbon–halogen (C–X) bonds are prevalent in organic compounds, and many organohalides are commercially available or readily synthesized, the formation of carbon radicals via the cleavage of C–X bonds is a useful transformation. Whereas the conventional methods to generate carbon radicals from C–X bonds relied on the use of stoichiometric amount of metal-based reagents such as SmI_2[2] or $SnBu_3H$/AIBN,[3] the light-mediated alternative process, in which the C–X bonds are cleaved in the presence of photocatalysts (PCs) upon irradiation, has drawn much attention due to its environmentally benign nature.[4]

Many research groups have reported light-mediated electron-transfer systems that induce C–X bond cleavage. However, most such studies employed substrates with C–I[5] or activated C–Br bonds, such as those with halogens at the benzylic position or α-position to carbonyl groups (Figure 1A).[6] In comparison, organochlorides tend to be cheaper and more widely available. Therefore, methods to activate the C–Cl bond for further transformation are highly desired. In photocatalytic electron transfer reactions, however,[7] only two examples of photochemical radical formation from "unactivated" aryl chlorides (that is, those bearing no electron withdrawing group) have been reported, due to the strongly negative reduction potential of aryl chlorides (e.g. E^{red} [PhCl/PhCl$^{\bullet-}$] = –2.88 V vs SCE) (Figure 1B).[8] Further, both cases utilized metal-containing PCs and the product yields were only moderate.[7b,9] In this report, we used UVA and visible light to generate carbon radicals from organochlorides, including unactivated ones, through single electron transfer using *N*-ethyl-3,6-bis(dimethylamino)carbazole (**CAR1**), a non-metal PC with a simple structure.

RESULTS AND DISCUSSION

Design and Property of Carbazole-Based Photocatalyst

Our lab has focused on photoredox reactions using PCs with carbazole as a central framework. Previously, we reported that a 3,6-dimethoxycarbazole derivative (**CAR3**, Scheme 1), which has an electron-deficient aryl substituent on the carbazole nitrogen, could catalyze the photochemical dehalogenation of unactivated primary alkyl bromides.[10] The fact that carbazole **CAR3** showed higher reducing ability than **CAR2** (Scheme 1) was rationalized by assuming that the charge-transfer (CT) excited state of **CAR3** effectively suppresses back electron transfer. However, the **CAR3** could not reduce some of the more demanding substrates, such as aryl bromides and organochlorides.

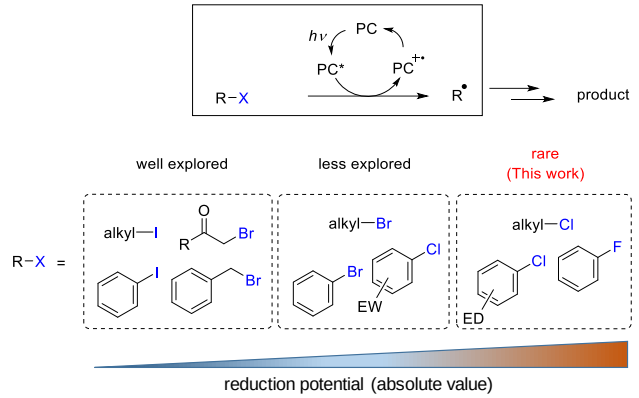

(A)

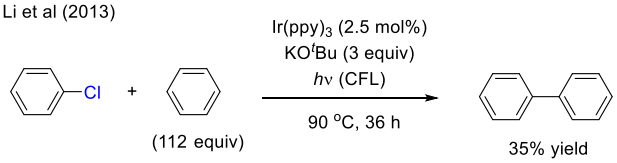

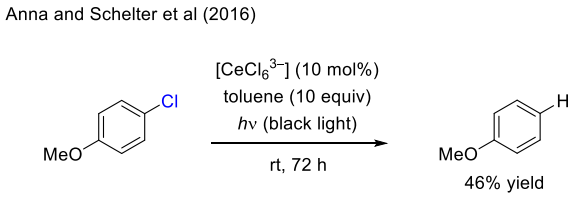

(B)

Figure 1. (A) Photo-induced radical generation from organohalides via single electron transfer. (B) Previously reported photocatalytic radical generation from unactivated aryl chlorides.

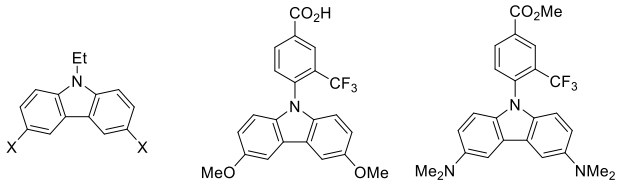

Scheme 1 Structures of related non-metal PCs

To design a better PC, we consider the following aspects. (1) Based on the Rehm-Weller equation,[11] a higher energy level in the highest occupied molecular orbital (HOMO) of the ground state PC (that is, a lower oxidation potential) and a higher excitation energy lead to better reducing ability in the excited PC species. (2) At the same time, the oxidation potential of the ground state PC should not be too low, so that the PC regeneration ($PC^{\bullet+} \rightarrow PC$) remains feasible. (3) The ideal PC should absorb photons at wavelengths longer than 350 nm, to avoid unwanted direct excitation of substrates and allow the utilization of the UVA and visible light region of sunlight. (4) Based on our previous finding,[10] the CT excited state helps to retard the unproductive back electron transfer.[12]

DFT calculation for the parent molecule (carbazole) showed large orbital coefficients at C3 and C6 in the HOMO, while nodes exist on these two carbons in the lowest unoccupied molecular orbital (LUMO) (Figure 2). This observation suggests that the introduction of electron-donating groups at C3 and C6 would raise the HOMO energy with minimal effect on the LUMO level, possibly leading to higher reducing ability in the excited PC species (vide supra) and redshifted light absorption. Therefore, we identified 3,6-diaminocarbazole (**CAR1**) as a promising PC with high reducing ability.

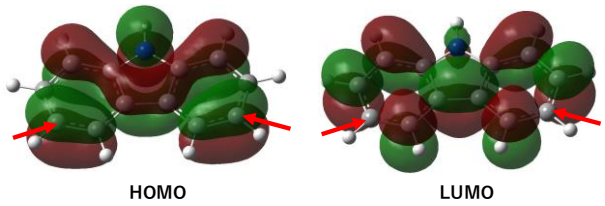

Figure 2. Frontier orbitals of carbazole calculated using DFT at B3LYP level of theory employing 6-31G(d,p) basis set. The C3 and C6 atoms are indicated by red arrows.

CAR1 was previously tested by Jamison et al.[13] as a candidate PC in the Saito deoxygenation reaction,[14] where it gave no product and was abandoned. **CAR1** can be readily synthesized from *N*-ethylcarbazole in two steps. Cyclic voltammetric analysis of **CAR1** revealed its oxidation potential to be +0.27 V vs SCE, which is 0.57 V lower than that of the dimethoxy-substituted variant **CAR2** (+0.84 V vs SCE) (Figure 3A). This could be attributed to the raised HOMO level of **CAR1** caused by the strong electron-donating NMe_2 groups, which was corroborated by the DFT calculation (Figure 3B and Figure S1). Experimental absorption spectra of **CAR1** and **CAR2** are compared in Figure 3C, together with vertical excitation energies calculated by time-dependent (TD)-DFT. Although the calculated bands displayed a systematic blue shift compared to the experimental spectra,[15] the good overall agreement between theory and experiment allowed an assignment of the electronic transitions. The lowest energy peak of **CAR1**, which is attributed to the HOMO → LUMO transition, reaches visible light region with wavelengths as long as 430 nm, while that of **CAR2** ends at only 390 nm. This observation is in good agreement with the calculation that indicates a smaller $S_0 \rightarrow S_1$ excitation energy for **CAR1** than **CAR2**. The bathochromic shift in the absorption spectrum of **CAR1** compared to **CAR2** (Figure 3B) can be ascribed to the increased HOMO energy level and the marginal change of the LUMO energy level by changing –OMe (**CAR2**) to $-NMe_2$ (**CAR1**). From the onset value of the fluorescence emission peak ($\lambda \approx 410$ nm, Figure 3D), the excited state of **CAR1** was estimated to be 3.02 eV above the ground state. According to the above data, the excited-state oxidation potential of **CAR1** could be approximated by E_{ox}^{*} [$\mathbf{CAR1}^{\bullet+}$/ **CAR1***] = –2.75 V vs SCE, using the Rehm-Weller equation. This value is comparable to the reduction potential of chlorobenzene.

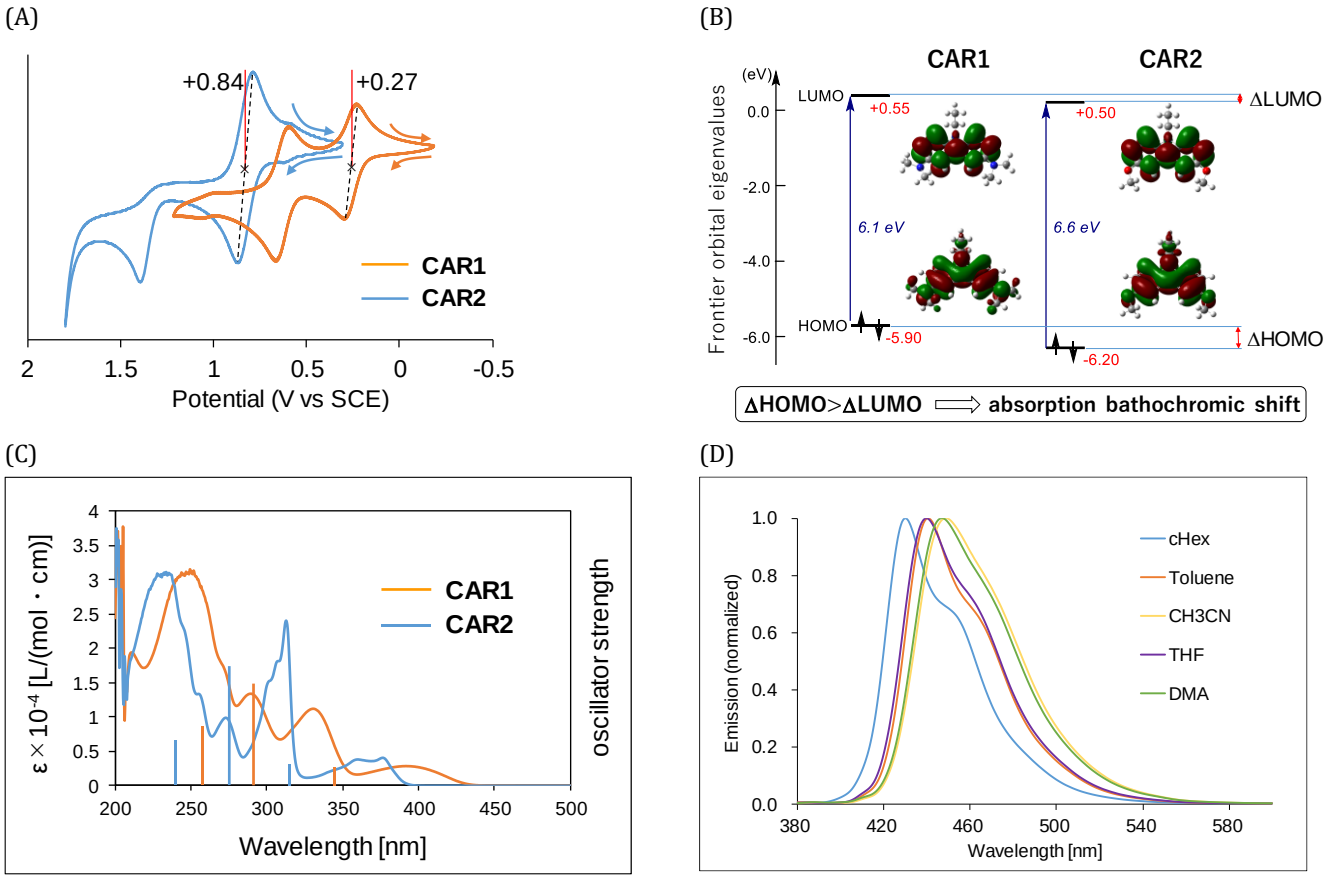

Figure 3. (A) Cyclic voltammograms of **CAR1** and **CAR2** (1.0×10^{-3} M in CH_3CN). (B) Comparison of the DFT-calculated frontier orbitals for **CAR1** and **CAR2**. (C) Experimental absorption spectra of **CAR1** (orange line) and **CAR2** (blue line), together with the vertical excitation energies for **CAR1** (orange bar) and **CAR2** (blue bar) calculated by TD-DFT. The height of bars corresponds to their oscillator strength. (D) Emission spectra of **CAR1** in various solvents. λ_{ex} = 365 nm.

The fluorescence emission spectrum of **CAR1** is slightly affected by the solvent polarity (Figure 3D), becoming more red-shifted and less well resolved when the solvent polarity increases. According to the Lippert-Mataga equation,[16] the dipole moment change ($\Delta\mu = \mu_e - \mu_g$) between the ground and excited states was estimated to be 4.83 D, which is larger than that of **CAR2** (3.46 D)(Table S2, Figure S2). The calculation showed that the S_1 excited state of **CAR1** has a much higher dipole moment than that of **CAR2**, in good agreement with the experimental data (Figure S3). These results indicate that the S_1 state of **CAR1** has a weak CT character.[17]

Carbazole-Catalyzed Generation of Carbon Radicals from Organohalides by Photo-Irradiation

For the photochemical radical generation from unactivated organochlorides, we first discuss the reduction of a primary alkyl chloride **1a**. The initial PC experiments conducted for **CAR1**–**CAR4** using UVA-LED irradiation (λ_{max} = 365 nm, 440 mW) with PC (5 mol%), 1,4-cyclohexadiene (CHD, 2 equiv) and Bu_3N (2 equiv) in THF revealed that only **CAR1** showed a catalytic activity (entries 1–4, Table 1). Fortunately, the use of high-polarity solvents dramatically increased the product yield (entries 5–7), with *N,N*-dimethylacetamide (DMA) being the optimal solvent (entry 7). This trend can be attributed to the solvation-assisted facile electron transfer from PC* to **1a**. The yield further increased when the base was changed from Bu_3N to $^iPr_2NEt$ (entry 8). When these optimal reaction conditions were applied to the photochemical reduction of an unactivated aryl chloride **3a**, the reduction product **4a** was formed at 51% yield (entry 9). **CAR2** again gave lower yield than **CAR1** (entry 10 vs. 9). Tertiary amine could be replaced by inorganic base K_2CO_3 without significant loss of reactivity (entry 11 vs 9), suggesting that tertiary amine does not play a key role in the catalyst regeneration but works just as a base in this reaction. This result does not contradict the fact that the oxidation potential of tertiary amine is higher than that of **CAR1** (vide supra). Varying the catalyst loading did not have a significant effect on the reaction rate (entries 12 vs 13), indicating that the reaction rate was limited by the light irradiation intensity. Indeed, when the irradiation power was doubled, the product yield changed from 51% to 86% (entries 14 vs 9), and no reaction occurred without light irradiation (entry 15).

Table 1. Optimization for the dehalogenation of unactivated aryl chloride[a] using different PCs

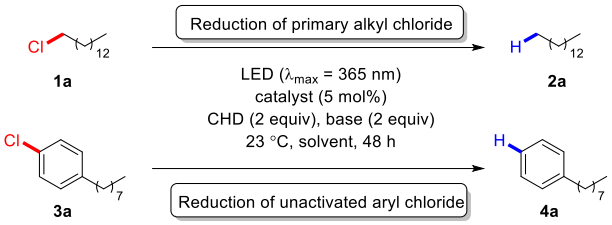

entry	substrate	PC	base	solvent	yield (%)
1	**1a**	**CAR1**	Bu_3N	THF	2
2	**1a**	**CAR2**	Bu_3N	THF	0
3	**1a**	**CAR3**	Bu_3N	THF	0
4	**1a**	**CAR4**	Bu_3N	THF	0
5	**1a**	**CAR1**	Bu_3N	DMF	21
6	**1a**	**CAR2**	Bu_3N	DMF	1
7	**1a**	**CAR1**	Bu_3N	DMA	45
8	**1a**	**CAR1**	$^iPr_2NEt$	DMA	63
9	**3a**	**CAR1**	$^iPr_2NEt$	DMA	51
10	**3a**	**CAR2**	$^iPr_2NEt$	DMA	10
11	**3a**	**CAR1**	K_2CO_3	DMA	45
12	**3a**	**CAR1**[b]	$^iPr_2NEt$	DMA	48
13	**3a**	**CAR1**[c]	$^iPr_2NEt$	DMA	44
14[d]	**3a**	**CAR1**	$^iPr_2NEt$	DMA	86
15[e]	**3a**	**CAR1**	$^iPr_2NEt$	DMA	0

[a] Conditions: substrate (0.18 mmol, 1 equiv), PC (5 mol%), CHD (2 equiv), base (2 equiv), solvent (0.1 M), UVA-LED (λ_{max} = 365 nm, 440 mW), argon atmosphere, 23 °C, GC yield shown (internal standard method). [b] 1 mol%. [c] 10 mol%. [d] UVA-LED (880 mW). [e] No light.

Next, we examined the substrate scope for photochemical reductions of organohalides using **CAR1**, and the results are summarized in Table 2. Aryl chlorides bearing no electron-withdrawing group (**3a–f**) afforded the reduced products in good-to-high yields regardless of the substitution positions, as seen in the results of **3c–e**. The exclusive formation of the cyclized product **5** from **3f** with a pendant olefin suggested that this reaction proceeded via aryl radical formation. Unsurprisingly, aryl chlorides having electron-withdrawing groups (**3g–i**) and π-extended systems (**3j** and **3k**) were better substrates for this reaction, giving corresponding products in high yields after shorter reaction times. The reduction of **3g** was also performed using a continuous flow system equipped with a quartz cell (4 cm × 1 cm × 0.1 cm) and an HPLC pump. A 0.02 M DMA solution of **3g** was passed through the cell (inner volume 0.4 mL) at a rate 0.2 mL/min under UVA-LED irradiation, affording the reduced product in 73% yield (residence time: 2 min). The visible light absorption of **CAR1** (λ = 400–500 nm, Figure 3C) allowed the reduction of **3j** and **3k** under visible light irradiation with high yields (83% and 91%, respectively). Sunlight-mediated reaction using **CAR1** was demonstrated (Figure 4), in which the products were obtained in acceptable yields. A fluoroarene **6** underwent the photochemical reduction albeit in a low yield.

Several alkyl halides were also examined. In addition to the primary alkyl chloride **1a**, secondary and tertiary alkyl chlorides (**1b** and **1c**, respectively) uneventfully gave the desired alkanes in good yields. The primary alkyl fluoride **7** did not react under this condition.

Table 2. Photochemical reductions of organohalides using CAR1[a]

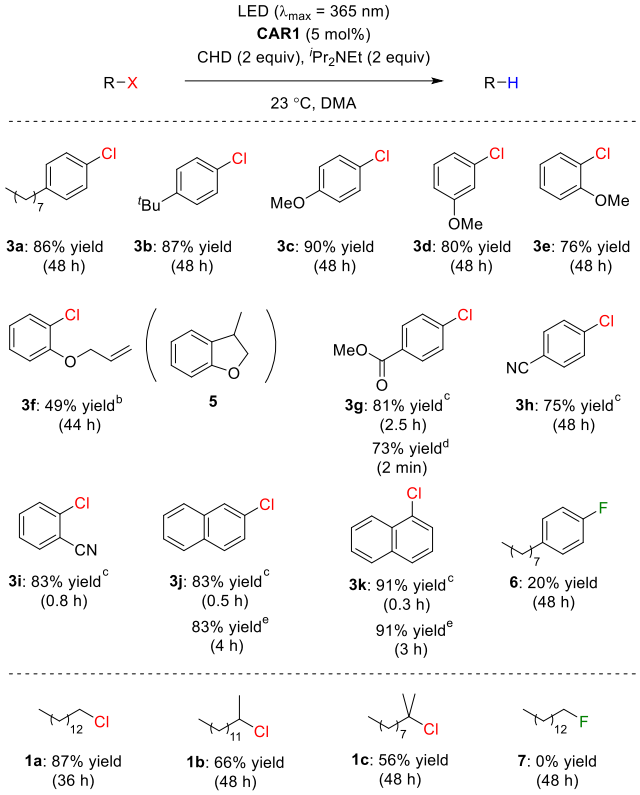

[a] Conditions: organohalides (0.18 mmol, 1 equiv), **CAR1** (5 mol%), CHD (2 equiv), $^iPr_2NEt$ (2 equiv), DMA (0.1 M), UVA-LED (880 mW), argon atmosphere, 23 °C, GC yield shown (internal standard method). [b] Isolated yield of **5**. [c] UVA-LED (440 mW). [d] Flow system (See Supporting Information). [e] Visible light (λ = 400–500 nm).

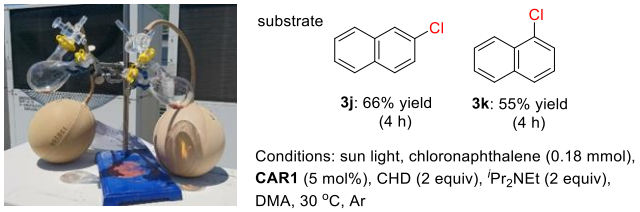

Figure 4. Sunlight-mediated reduction of chloronaphthalenes using **CAR1**. The yields of product (naphthalene) were determined by GC analysis.

Table 3. Photochemical coupling reactions of aryl chlorides with (hetero)arenes[a]

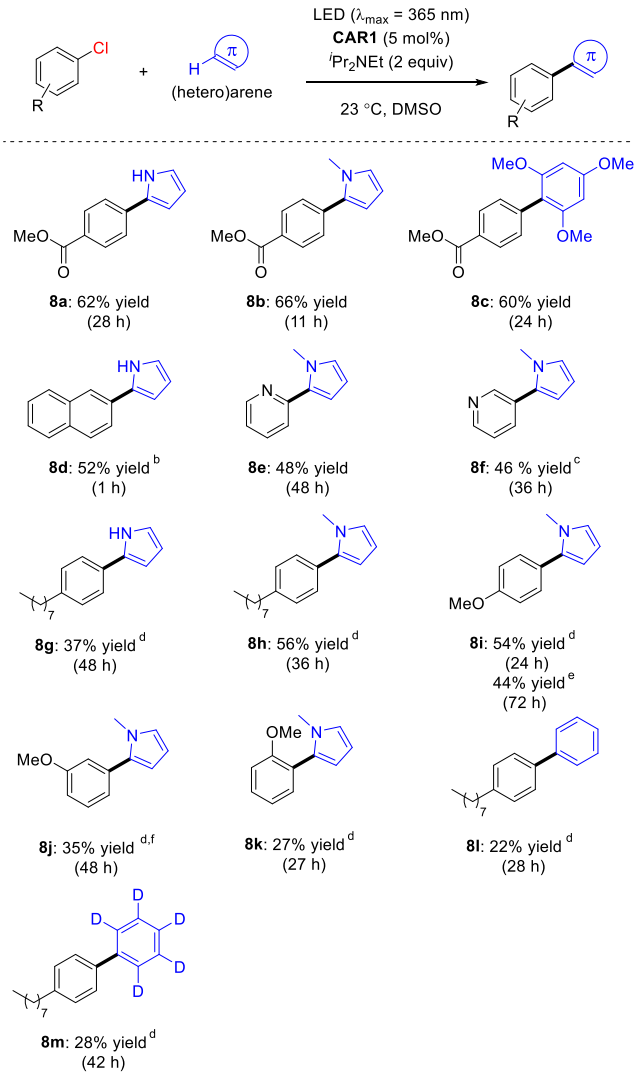

[a] Conditions: aryl chloride (0.18 mmol, 1 equiv), (hetero)arene (20 equiv), **CAR1** (5 mol%), ^{i}Pr$_2$NEt (2 equiv), DMSO (0.1 M), UVA-LED (440 mW), argon atmosphere, 23 °C, isolated yield shown. [b] K_2CO_3 (2 equiv) instead of ^{i}Pr$_2$NEt. [c] UVA-LED (880 mW). [d] aryl chloride (0.18 mmol, 1 equiv), (hetero)arene (0.9 mL), **CAR1** (5 mol%), K_2CO_3 (2 equiv), DMSO (0.9 mL), UVA-LED (880 mW), argon atmosphere, 90 °C. [e] Visible light (400—500 nm). [f] NMR yield using durene as an internal standard.

We then turned our attention to the C–C bond forming reactions utilizing the developed catalytic system of **CAR1**. Judicious choice of coupling partner and reaction condition was necessary to permit the addition reaction of the aryl radical (which has a short lifetime) and suppress its competitive hydrogen abstraction. Similar to the reactions developed by König et al.,[8a,8b] the photochemical coupling reaction of electron-deficient aryl chlorides with electron-rich (hetero)arenes could be realized using 5 mol% of **CAR1** (**8a–d**). The omission of CHD and the use of DMSO instead of DMA were the keys to suppress the formation of reduction product, because both CHD and DMA are potential hydrogen atom donors. Chloropyridines could also serve as a radical donor to form the pyridine adducts **8e–f** in acceptable yields. Unsurprisingly, unactivated (electronically neutral) aryl chlorides gave adducts in low yields (<10%) under the same reaction conditions. However, an increased temperature (90 °C) increased the yields from these challenging substrates. In addition, the use of inorganic base instead of organic base and excess amount of radical acceptors were effective, probably due to the suppression of competitive hydrogen abstraction of the aryl radicals. Under the optimized conditions, electronically neutral arene adducts with pyrroles (**8g–k**) were obtained. Visible light irradiation also gave the C–C bond formation product (44% yield for **8i**). Benzene adduct and its deuterated variant **8l** and **8m** were generated in moderate yields.[18]

Mechanistic Observations

The fluorescence quenching method has often been used to gain insight into reaction mechanisms. Electron transfer involving a photocatalyst in singlet excited state leads to a reduction (i.e., quenching) of fluorescence from the photocatalyst. The quenching rate constant (k_q) can be obtained by measuring fluorescence intensity in the presence of various concentrations of quenchers by means of the Stern-Volmer equation:

$$\frac{I_0}{I} = 1 + k_q \tau_s [Q]$$

where I_0 and I are the fluorescence intensities in the absence and presence of quencher, respectively; τ_s is the lifetime of the singlet excited state; and [Q] is the quencher concentration. In this study, three different quenchers were used: 1-chloronaphthalene (**3k,** an activated aryl chloride), PhCl (an unactivated aryl chloride), and ^{i}PrNEt$_2$ (a potential reductant). From the results (Figure 5), **3k** exhibits strong quenching effects. The other two quenchers had weaker effects.

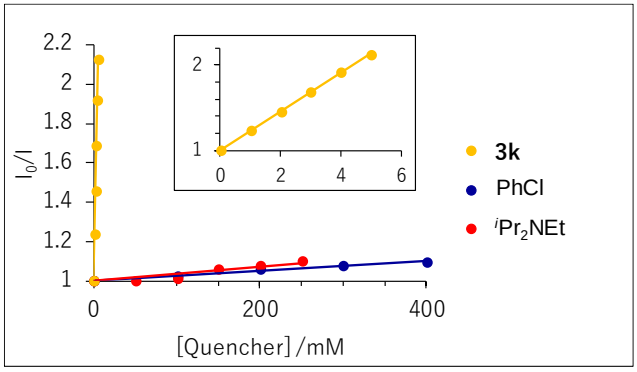

Figure 5. Fluorescence quenching of **CAR1** in the presence of varying concentrations of **3k**, PhCl, or ^{i}Pr$_2$NEt as quenchers. The quenching rate constants (k_q) according to the Stern-Volmer equation are 1.33×10^{10}, 1.53×10^{7}, and 2.16×10^{7} M^{-1} s^{-1}, respectively. The fluorescence lifetime of **CAR1** in THF was determined to be τ = 17.1 ns by the photoluminescence decay measurement (Figure S6) and used for the k_q calculation. Measurements were performed with 5 μM of **CAR1** in THF for **3k**, and in DMA for PhCl and ^{i}Pr$_2$NEt. Inset: magnification of the low concentration region for **3k**.

To test whether any radical-chain mechanism is operative in this reaction (meaning that the photosensitized **CAR1** merely works as an initiator), substrate **3g** was subjected to the "light/dark experiment", i.e. photochemical reduction with intermittent irradiation with 30-min ON followed by 10-min OFF in one cycle. Figure 6 shows no reaction progress during the light-OFF periods, which implies that a radical-chain mechanism is unlikely in our system.[19]

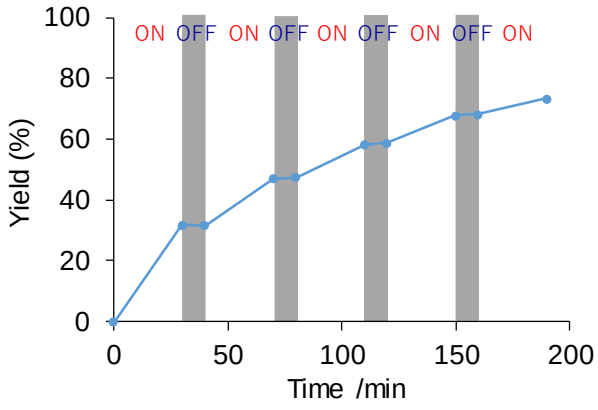

Figure 6. Progress of photochemical reduction of **3g** using **CAR1** under intermittent irradiation. Reaction conditions are identical to those in Table 2.

Based on the above experimental findings, a catalytic mechanism of the photochemical reactions of organohalide using **CAR1** was proposed, as shown in Figure 7 (using aryl chloride as a representative example). The excited singlet **CAR1** (**^{1}CAR***) with a highly negative oxidation potential (E^* = –2.75 V vs SCE) transfers one electron to aryl chloride (oxidative quenching cycle) to form an aryl radical (Ar$^\bullet$),[20] which abstracts a hydrogen atom from CHD or other solvent to afford the reduced product (Ar–H). In the absence of reactive hydrogen atom donor, Ar$^\bullet$ can react with an electron-rich (hetero)arene to generate the radical adduct **11**, which is converted to the coupling product **12**. **CAR1$^{\bullet+}$** accepts an electron from **9**, **11**, or amine to regenerate **CAR1**, thus the catalytic cycle is completed. Alternatively, for the reduction of unactivated aryl chlorides in the presence of ^{i}Pr$_2$NEt, we could not rule out a reductive quenching cycle. In this reductive cycle, **^{1}CAR*** accepts an electron from ^{i}Pr$_2$NEt to generate **CAR1$^{\bullet-}$**, which transfers an electron to the aryl chloride. Results of the "light/dark" experiment indicate that a radical-chain process is unlikely in this system. This experimental conclusion is also reasonable because an electron transfer from **9** or **11** to an aryl chloride, which is necessary for the radical-chain propagation, is thermodynamically unfeasible.[21]

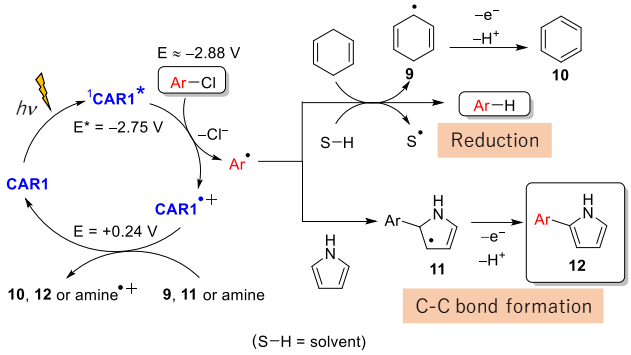

Figure 7. Plausible catalytic mechanism of **CAR1**.

CONCLUSION

A bis(dimethylamino)carbazole (**CAR1**) was found to catalytically function as a photoreductant to generate carbon radicals from organochlorides. It is a structurally simple organic molecule with no metals, and can be readily and cheaply synthesized. Due to its two strong electron-donating NMe$_2$ groups, **CAR1** has an exceptionally high reducing ability upon irradiation. Spectroscopic and electrochemical data showed that the oxidation potential of its excited state reaches as low as –2.75 V vs SCE. Using **CAR1** as a PC, various types of organohalides could undergo photochemical reduction, including unactivated (i.e. without electron-withdrawing substituents adjacent to halides) alkyl chlorides and aryl chlorides. C–C bond formation with electron-rich (hetero)arenes was also possible. Another benefit of the NMe$_2$ groups is the redshift of absorption bands to reach the visible region, allowing the employment of visible light irradiation or even sunlight in place of UVA light. The experimental results were consistent with the assumption that the aryl radical is generated from the aryl chloride in this reaction, and a plausible catalytic mechanism was proposed.

Despite the recent explosive development of photosensitization reactions, PCs with high reducing ability are still rare, let alone those that function under visible light.[22] The development of such reduction-based reactions for more difficult substrates is underway in our laboratory.

EXPERIMENTAL SECTION

General All reactions were carried out in well cleaned and oven-dried glassware with magnetic stirring. Operations were performed under an atmosphere of dry argon using Schlenk and vacuum techniques. Melting points were measured on a Yanaco MP-500D and are not corrected. ^{1}H and ^{13}C NMR spectra (400 and 100 MHz, respectively) were recorded on a Bruker Avance III HD 400 using TMS (0 ppm) and CDCl$_3$ (77.0 ppm) in CDCl$_3$ and residual acetone (2.05 ppm) and CD$_3$COCD$_3$ (29.84 ppm) in acetone-d$_6$ as an internal standard, respectively. The following abbreviations are used in connection with NMR; s = singlet, d = doublet, t = triplet, q = quartet and m = multiplet. Mass spectra were measured using a JEOL JMS=T100LP (DART method, ambient ionization). GC analyses were performed using a Shimazu GC-2025 gas chromatograph equipped with GL Science Inertcap 5. Preparative column chromatography was performed using Kanto Chemical silica gel 60 N (spherical,

neutral). Thin layer chromatography (TLC) was carried out on Merk 25 TLC silica gel 60 F_{254} aluminium sheets. All starting materials were obtained from commercial sources unless otherwise noted. Carbazole **CAR1**,[23] **CAR2**,[23] **CAR3**[10], and aryl chloride **3f**[24] are known in the literature and synthesized according to the reported method. Substrate **3f** was synthesized according to the reported method. All the calculations were carried out using Gaussian 09.[25]

Spectral measurement Photoluminescence spectra were recorded on a spectrofluorometer (Jasco FP-6500) with a quartz absorption cuvette (light path: 1 cm). UV–visible spectra were recorded on a Shimadzu UV-1800 spetrometer with a quartz absorption cuvette (light path: 1 cm).

Redox property Cyclic voltammetric measurements were performed at 298 K, using an ALS CHI606S electrochemical analyzer, by using a solvent deaerated by Ar bubbling for 30 min before each measurement. The supporting electrolyte was 0.10 M $TBAClO_4$. A conventional three-electrode cell was used with a platinum working electrode and a platinum wire as a counter electrode. The cyclic voltammograms were recorded with respect to the $Ag/AgNO_3$ (10 mM) reference electrode at a sweep rate of 100 mV/s. The reduction or oxidation potentials (determined as the peak potentials) were corrected to the SCE scale on the basis of the measurement of the redox potential of the Fc/Fc+ couple as the standard (+0.43 V vs SCE)[26].

3,6-Bis(dimethylamino)-9H-carbazole To a 500 mL three-necked flask, 3,6-dibromocarbazole (6.0 g, 18.4 mmol, 1.0 equiv), dimethylamine hydrochloride (3.6 g, 44.4 mmol, 2.4 equiv), $Pd_2(dba)_3$ (0.17 g, 0.185 mmol, 1.0 mol%), Ruphos (0.205 g, 0.440 mmol, 2.4 mol%), and a THF solution of LiHMDS (1.3 M, 82 mL, 107 mmol, 5.8 equiv) were added in this order. The mixture was heated at 100 °C for 21 h, then dimethylamine hydrochloride (0.90 g, 11.1 mmol, 0.6 equiv) and a THF solution of LiHMDS (1.3 M, 20 mL, 27 mmol, 1.45 equiv) were added. The mixture was heated at 100 °C for 3 h. The resultant mixture was poured into 1 M HCl aq. (130 mL), then sat. $NaHCO_3$ aq. (130 mL) was added. The mixture was concentrated by a rotary evaporator. The residue was extracted with ethyl acetate thrice, dried over anhydrous $MgSO_4$, and filtered. The filtrate thus obtained was concentrated in vacuo. The residual solid was slurried in hexane/ethyl acetate mixed solvent (10 : 1) and filtered. The solid was again slurried in hexane/ethyl acetate mixed solvent (5 : 1) and filtered. The solid thus obtained was purified by chromatography on silica gel (hexane/ethyl acetate/Et_3N = 100/20/0.2) to give the product (3.33 g, 71% yield). Green solid. Mp 134.4–134.6 °C ; ^{1}H NMR (400 MHz, Acetone-d_6): δ = 9.56 (s, 1H), 7.49 (d, *J* = 2.4 Hz, 2H), 7.30 (d, *J* = 8.8 Hz, 2H), 7.00 (dd, *J* = 8.8, 2.4 Hz, 2H), 2.93 (s, 12H); ^{13}C NMR (100 MHz, Acetone-d_6): δ = 146.1, 135.6, 124.8, 115.9, 111.9, 105.3, 42.8; IR (neat): 3100, 3014, 2841, 1609, 1567, 1496, 1440, 1432, 1327, 1308, 1240, 1225, 1191, 1160, 1138, 1110, 938, 851, 822, 800, 789, 728, 678, 645 cm^{-1}; HRMS (DART): m/z calcd for $C_{16}H_{20}N_3$: 254.1652 [M+H$^+$]; found: 254.1657.

Methyl 4-(3,6-bis(dimethylamino)-9H-carbazol-9-yl)-3-trifluoromethylbenzoate (CAR4) K_3PO_4 (385.8 mg, 1.82 mmol, 3.0 equiv) was added to a sealed tube and flame-dried under vacuum. CuI (23.1 mg, 0.12 mmol, 0.2 equiv), *N,N*-dimethyl-1,2-ethandiamine (19.6 μL、0.18 mmol, 0.3 equiv) and THF (2.2 mL) were added. The mixture was stirred for 10 min at rt. Methyl 4-iodo-3-(trifluoromethyl)benzoate (200 mg, 0.61 mmol, 1.0 equiv) and 3,6-bis(dimethylamino)carbazole (230.2 mg, 0.91 mmol, 1.5 equiv) were added and the mixture was heated at 80 ℃ for 18 h. The reaction mixture was cooled to rt, then ethyl acetate was added. The resultant mixture was washed with brine four times, dried over anhydrous Na_2SO_4, and filtered. The filtrate was concentrated in vacuo and purified by chromatography on SiO_2 to give the product (42 mg, 15% yield). Red oil. ^{1}H NMR (400 MHz, $CDCl_3$): δ = 8.61 (d, *J* = 1.6 Hz, 1H), 8.34 (dd, *J* = 8.4, 2.0 Hz, 1H), 7.44 (d, *J* = 2.4 Hz, 2H), 7.39 (d, *J* = 8.0 Hz, 1H), 6.95 (dd, *J* = 9.0, 2.6 Hz, 2H), 6.71 (d, *J* = 8.8 Hz, 2H), 4.02 (s, 3H), 3.01 (s, 12H); ^{13}C NMR (100 MHz, $CDCl_3$): δ = 165.3, 146.0, 141.8, 137.3, 134.4, 132.7, 131.1 (q, $J_{C\text{-}F}$ = 31 Hz), 130.5, 129.0 (q, $J_{C\text{-}F}$ = 5 Hz), 124.6, 122.7 (q, $J_{C\text{-}F}$ = 273 Hz), 114.9, 110.4, 104.3, 52.8, 42.5; IR (neat): 2954, 2872, 2834, 2786, 1726, 1614, 1576, 1496, 1475, 1436, 1322, 1253, 1227, 1164, 1131, 1054, 965, 945, 923, 831, 795, 751, 731, 702, 662, 655, 598 cm^{-1}; HRMS (DART): m/z calcd for $C_{25}H_{25}F_3N_3O_2$: 456.1899 [M+H$^+$]; found: 456.1930.

General procedure of photochemical reductions of organohalides using CAR1 (Table 2) To a pyrex glassware were added alkyl or aryl halide (0.18 mmol, 1.0 equiv), **CAR1** (2.5 mg, 9 μmol, 5 mol%), 1,4-cyclohexadiene (33.7 μL, 0.36 mmol, 2 equiv), ^{i}Pr$_2$NEt (61.5 μL, 0.36 mmol, 2 equiv), pentadecane (internal standard for GC analysis, 30 μL) and DMA (1.8 mL). The mixture was deaerated by bubbling of argon for 10 min. The mixture was irradiated with two or four LED lamps (total 440 or 880 mW, respectively) at 23 °C for the indicated time (see the main text). Due to the volatility of the products, the yield of the product was determined by GC analysis based on the ratio of product to pentadecane except the reaction of **3f**, in which compound **5** was isolated by chromatography.

2,3-Dihydroxy-3-methylbenzofurane (5)[27] To a pyrex glassware were added 1-alloxy-2-chlorobenzene (**3f**, 27.0 μL, 0.18 mmol, 1.0 equiv), **CAR1** (2.5 mg, 9 μmol, 5 mol%), 1,4-cyclohexadiene (33.7 μL, 0.36 mmol, 2 equiv), ^{i}Pr$_2$NEt (61.5 μL, 0.36 mmol, 2 equiv), pentadecane (internal standard for GC analysis, 30 μL) and DMA (1.8 mL). The mixture was deaerated by bubbling of argon for 10 min. The mixture was irradiated with two or four LED lamps (total 440 or 880 mW, respectively) at 23 °C for 44 h. The reaction mixture was cooled to rt, then ethyl acetate was added. The resultant mixture was washed with brine once and water thrice, dried over anhydrous Na_2SO_4, and filtered. The filtrate was concentrated in vacuo and purified by chromatography on SiO_2 to give **5** (11.4 mg, 49% yield).

Photochemical reductions using visible light (for 3j and 3k) To a pyrex glassware were added alkyl or aryl halide (0.18 mmol, 1.0 equiv), **CAR1** (2.5 mg, 9 μmol, 5 mol%), 1,4-cyclohexadiene (33.7 μL, 0.36 mmol, 2 equiv), ^{i}Pr$_2$NEt (61.5 μL, 0.36 mmol, 2 equiv), pentadecane (internal standard for GC analysis, 30 μL) and DMA (1.8 mL). The mixture was deaerated by bubbling of argon for 10 min. The mixture was irradiated with 400–500 nm light (a 300W Xenon lamp, Asahi Spectra MAX-303 equipped with a 300- to 600-nm ultraviolet-visible module, and a combination of a 400-nm

long-pass and 500-nm short-pass filters) at 23 °C for the indicated time (see the main text). Due to the volatility of the products, the yield of the product was determined by GC analysis based on the ratio of product to pentadecane.

Photochemical reduction of 3g under flow system The flow-system equipment was manually assembled with a HPLC double-plunger pump, fluorinated transparent plastic tubes, a quartz flow-cell (0.1 × 1.0 × 4.0 cm), and four LED lamps. The overview of the system is shown SI (Figure S4 and S5). A deaerated DMA solution of **3g** (1.0 equiv, 20 mM), **CAR1** (5 mol%, 1 mM), 1,4-cyclohexadiene (2.0 equiv, 40 mM), $^{i}Pr_2NEt$ (2.0 equiv, 40 mM) and pentadecane (internal standard, 0.5 v/v%) was passed through the quartz cell at 0.2 mL/min flow rate with irradiation. Because the inner volume of the cell is 0.4 mL, the residence time is 2 min. After the steady state was reached the aliquot of the output solution was analyzed by GC, revealing that the yield of the desired product was 73% yield.

Sun light-mediated photochemical reductions (Figure 4) To a 100 mL two-necked round-bottomed flask were added naphthalene chloride **3j** or **3k** (0.18 mmol, 1.0 equiv), **CAR1** (2.5 mg, 9 μmol, 5 mol%), 1,4-cyclohexadiene (33.7 μL, 0.36 mmol, 2 equiv), $^{i}Pr_2NEt$ (61.5 μL, 0.36 mmol, 2 equiv), pentadecane (internal standard for GC analysis, 30 μL) and DMA (1.8 mL). The mixture was deaerated by bubbling of argon for 10 min. The mixture was stood without stirring on the roof of the building on May 13th, 2017 (the outside temperature was 30 °C) for the indicated time. The reaction was monitored by GC analysis. The yield of the product was determined by GC analysis based on the ratio of product to pentadecane.

Photochemical coupling reactions of aryl chlorides with (hetero)arenes (Table 3) (Procedure A) To a pyrex glassware were added aryl chloride (0.18 mmol, 1.0 equiv), (hetero)arene (3.6 mmol, 20 equiv), **CAR1** (2.5 mg, 9 μmol, 5 mol%), $^{i}Pr_2NEt$ (61.5 μL, 0.36 mmol, 2 equiv) and DMSO (1.8 mL). The mixture was deaerated by bubbling of argon for 10 min. The mixture was irradiated with two LED lamps (total 440 mW) at 23 °C for the indicated time (see the main text). Then brine was added to the reaction mixture to quench the reaction. The resultant mixture was extracted with Et_2O thrice, dried over anhydrous Na_2SO_4, and filtered. The filtrate was concentrated in vacuo and purified by chromatography on SiO_2 to afford the product.

(Procedure B) To a pyrex glassware were added aryl chloride (0.18 mmol, 1.0 equiv), (hetero)arene (3.6 mmol, 20 equiv), **CAR1** (2.5 mg, 9 μmol, 5 mol%), $^{i}Pr_2NEt$ (61.5 μL, 0.36 mmol, 2 equiv) and DMSO (1.8 mL). The mixture was deaerated by bubbling of argon for 10 min. The mixture was irradiated with two or four LED lamps (total 440 mW or 880 mW, respectively) at 23 °C for the indicated time (see the main text). Then brine was added to the reaction mixture to quench the reaction. The resultant mixture was extracted with EtOAc thrice, dried over anhydrous Na_2SO_4, and filtered. The filtrate was concentrated in vacuo and purified by chromatography on SiO_2 to afford the product.

(Procedure C) To a pyrex glassware were added aryl chloride (0.18 mmol, 1.0 equiv), (hetero)arene (0.9 mL, 56–73 equiv), **CAR1** (2.5 mg, 9 μmol, 5 mol%), K_2CO_3 (49.8 mg, 0.36 mmol, 2 equiv) and DMSO (0.9 mL). The mixture was deaerated by bubbling of argon for 10 min. The mixture was irradiated with four LED lamps (total 880 mW) at 90 °C for the indicated time (see the main text). Then brine was added to the reaction mixture to quench the reaction. The resultant mixture was extracted with Et_2O thrice, dried over anhydrous Na_2SO_4, and filtered. The filtrate was concentrated in vacuo and purified by chromatography on SiO_2 to afford the product.

Methyl 4-(1H-pyrrol-2-yl)benzoate (8a)[28] Procedure A. 22.3 mg, 62% yield, white solid.

Methyl 4-(1-methyl-1H-pyrrol-2-yl)benzoate (8b)[28] Procedure A. 25.5 mg, 66% yield, white solid.

Methyl 4-(2,4,6-trimethoxyphenyl)benzoate (8c)[28] Procedure A. 32.9 mg, 60% yield, white solid.

2-(2-Naphthalenyl)-1H-pyrrole (8d)[29] Procedure A. 18.0 mg, 52%, yellow solid.

2-(1-Methyl-1H-pyrrol-2-yl)pyridine (8e)[30] Procedure B. Irradiated with the LED lamps (total 440 mW). 13.8 mg, 48%, yellow oil.

3-(1-Methyl-1H-pyrrol-2-yl)pyridine (8f)[31] Procedure B. Irradiated with the LED lamps (total 880 mW). 13.2 mg, 46%, yellow oil.

2-(4-Octylphenyl)-1H-pyrrole (8g) Procedure C. 16.7 mg, 37% yield, white solid. Mp 69.5–70.0 °C; ^{1}H NMR (400 MHz, $CDCl_3$): δ = 8.39 (s, 1H), 7.39 (d, *J* = 8.4 Hz, 2H), 7.18 (d, *J* = 8.4 Hz, 2H), 6.78 (m, 1H), 6.48 (m, 1H), 6.29 (q, *J* = 2.9 Hz, 1H), 2.59 (t, *J* = 7.8 Hz, 2H), 1.61 (m, 2H), 1.31–1.27 (m, 10H), 0.88 (t, *J* = 6.8 Hz, 3H); ^{13}C NMR (100 MHz, $CDCl_3$): δ = 141.0, 132.3, 130.2, 128.9, 123.8, 118.4, 109.9, 105.4, 35.6, 31.9, 31.5, 29.5, 29.3, 29.3, 22.7, 14.1; IR (neat): 3395, 2950, 2918, 2848, 1507, 1463, 1126, 1108, 1031, 823, 796, 782, 732, 718, 559, 526 cm^{-1}; HRMS (ESI): m/z calcd for $C_{18}H_{26}N$: 256.2065 [M+H$^+$]; found: 256.2093.

1-Methyl-2-(4-octylphenyl)-1H-pyrrole (8h) Procedure C. 27.2 mg, 56% yield, yellow oil. ^{1}H NMR (400 MHz, $CDCl_3$): δ = 7.31 (dt, *J* = 8.1, 1.9 Hz, 2H), 7.20 (d, *J* = 8.0 Hz, 2H), 6.70 (t, *J* = 2.2 Hz, 1H), 6.21–6.18 (m, 2H), 3.66 (s, 3H), 2.62 (t, *J* = 7.8 Hz, 2H), 1.64 (m, 2H), 1.33–1.28 (m, 10H), 0.88 (t, *J* = 7.0 Hz, 3H); ^{13}C NMR (100 MHz, $CDCl_3$): δ = 141.6, 134.7, 130.6, 128.5, 128.3, 123.3, 108.2, 107.6, 35.7, 35.0, 31.9, 31.5, 29.5, 29.4, 29.3, 22.7, 14.1; IR (neat): 2922, 2852, 1505, 1475, 1414, 1309, 1240, 1089, 1056, 1015, 982, 838, 777, 705, 606, 547 cm^{-1}; HRMS (ESI): m/z calcd for $C_{19}H_{28}N$: 270.2222 [M+H$^+$]; found: 270.2246.

1-Methyl-2-(4-methoxyphenyl)-1H-pyrrole (8i)[32] Procedure C. 18.3 mg, 54% yield, colorless oil.

1-Methyl -2-(3-methoxyphenyl)-1H-pyrrole (8j)[32] Procedure C. 12.0 mg, 35% yield, colorless oil.

1-Methyl-2-(2-methoxyphenyl)-1H-pyrrole (8k)[33] Procedure C. 9.0 mg, 27% yield, colorless oil.

4-Octyl-1,1'-biphenyl (8l)[34] Procedure C. 10.4 mg, 22% yield, white solid.

4-Octyl(2',3',4',5',6'-$^2H_5$)-1,1'-biphenyl (8m) Procedure C. 13.6 mg, 28% yield, white solid. Mp 38.5–39.2 °C; ^{1}H NMR (400 MHz, $CDCl_3$): δ = 7.51 (d, *J* = 8 Hz, 2H), 7.25 (d, *J* = 8.4 Hz, 2H), 2.64 (t, *J* = 7.6 Hz, 2H), 1.65 (m, 2H), 1.33-1.28 (m, 10H), 0.88 (t, *J* = 7.2 Hz, 3H); ^{13}C NMR (100 MHz, $CDCl_3$): δ = 142.1, 141.0, 138.5, 128.8, 128.7 (t, *J* = 18 Hz), 128.2 (t,

24 Hz), 126.9, 126.5 (t, J = 24 Hz), 35.6, 31.9, 31.5, 29.5, 29.4, 29.3, 22.7, 14.1; IR (neat): 2955, 2918, 2848, 1515, 1465, 1381, 1332, 1135, 1019, 992, 862, 834, 815, 762, 721, 635, 552 cm^{-1}; HRMS (DART): m/z calcd $C_{20}H_{22}D_5$: 272.2421 [M+H$^+$]; found: 272.2427.

Visible light-mediated photochemical coupling reactions of 3c with N-methylpyrrole (synthesis of 8i) To a pyrex glassware were added **3c** (0.18 mmol, 1.0 equiv), *N*-methylpyrrole (0.9 mL, 56 equiv), **CAR1** (2.5 mg, 9 μmol, 5 mol%), K_2CO_3 (49.8 mg, 0.36 mmol, 2 equiv) and DMSO (0.9 mL). The mixture was deaerated by bubbling of argon for 10 min. The mixture was irradiated with 400–500 nm light (a 300W Xenon lamp, Asahi Spectra MAX-303 equipped with a 300- to 600-nm ultraviolet-visible module, and a combination of a 400-nm long-pass and 500-nm short-pass filters) at 90 °C for 72 h. Then brine was added to the reaction mixture to quench the reaction. The resultant mixture was extracted with Et_2O thrice, dried over anhydrous Na_2SO_4, and filtered. The filtrate was concentrated in vacuo and purified by chromatography on SiO_2 to afford the product **8i** (44% yield).

Light/dark experiment (Figure 6) To a pyrex glassware were added **3g** (0.18 mmol, 1.0 equiv), **CAR1** (2.5 mg, 9 μmol, 5 mol%), 1,4-cyclohexadiene (35.0 mg, 0.36 mmol, 2 equiv), ^{i}Pr$_2$NEt (61.5 μL, 0.36 mmol, 2 equiv), pentadecane (internal standard for GC analysis, 30 μL) and DMA (1.8 mL). The mixture was deaerated by bubbling of argon for 10 min. The mixture was subjected to ON/OFF rotations of irradiation with two LED lamps (30 min-ON followed by 10 min-OFF for one cycle) at 23 °C. The reaction progress was monitored by GC analysis of the aliquots taken out of the reaction at intervals. The yield was determined based on the ratio of product to pentadecane.

ASSOCIATED CONTENT

Supporting Information.

Experimental procedures, theoretical calculation data and ^{1}H and ^{13}C NMR spectra (PDF)

This material is available free of charge via the Internet at http://pubs.acs.org.

AUTHOR INFORMATION

Corresponding Author

* matsubara.ryosuke@people.kobe-u.ac.jp

ACKNOWLEDGMENT

This work was carried out by the joint research program of Molecular Photoscience Research Center, Kobe University (H29001). We thank Profs. Atsunori Mori and Kentaro Okano in Kobe University for their help on mass analysis. Financial supports from JSPS KAKENHI Grant Number JP16K18844, Shorai Foundation for Science and Technology, and Research Foundation for Opto-Science and Technology are greatly appreciated. This work was also supported by the Ministry of Education, Culture, Sports, Science and Technology (MEXT), Japan, and by Special Coordination Funds for Promoting Science and Technology, Creation of Innovation Centers for Advanced Interdisciplinary Research Areas (Innovative Bioproduction Kobe), MEXT, Japan.

REFERENCES

[1] For a recent review, see: Studer, A.; Curran, D. P. Catalysis of Radical Reactions: A Radical Chemistry Perspective. Catalysis of Radical Reactions: A Radical Chemistry Perspective. *Angew. Chem. Int. Ed*. **2016**, *55*, 58–102.

[2] Szostak, M.; Fazakerley, N. J.; Parmar, D.; Procter, D. J. Cross-Coupling Reactions using Samarium(II) Iodide. *Chem. Rev.* **2014**, *114*, 5959–6039, and references therein.

[3] (a) Curran, D. P. The Design and Application of Free Radical Chain Reactions in Organic Synthesis. Part 1. *Synthesis* **1988**, 417–439; (b) Curran, D. P. The Design and Application of Free Radical Chain Reactions in Organic Synthesis. Part 2. *Synthesis* **1988**, 489–513.

[4] For recent reviews of photocatalytic reactions, see: (a) Prier C, K.; Rankic, D. A.; MacMillan, D. W. C. Visible Light Photoredox Catalysis with Transition Metal Complexes: Applications in Organic Synthesis. *Chem. Rev*. **2013**, *113*, 5322–5363; (b) Narayanam, J. M. R.; Stephenson, C. R. J. Visible Light Photoredox Catalysis: Applications in Organic Synthesis. *Chem. Soc. Rev*. **2011**, *40*, 102–113; (c) Skubi, K. L.; Blum, T. R.; Yoon, T. P. Dual Catalysis Strategies in Photochemical Synthesis. *Chem. Rev*. **2016**, *116*, 10035–10074.

[5] Selected examples: (a) Nguyen, J. D.; D'Amato, E. M.; Narayanam, J. M. R.; Stephenson, C. R. J. Engaging Unactivated Alkyl, Alkenyl and Aryl Iodides in Visible-Light-Mediated Free Radical Reactions. *Nature Chem*. **2012**, *4*, 854; (b) Kim, H.; Lee, C. Visible-Light-Induced Photocatalytic Reductive Transformations of Organohalides. *Angew. Chem. Int. Ed*. **2012**, *51*, 12303–12306.

[6] Selected examples: (a) Su, Y.; Zhang, L.; Jiao, N. Utilization of Natural Sunlight and Air in the Aerobic Oxidation of Benzyl Halides. *Org. Lett*. **2011**, *13*, 2168–2171; (b) Nicewicz, D. A.; MacMillan, D. W. C. Merging Photoredox Catalysis with Organocatalysis: The Direct Asymmetric Alkylation of Aldehydes. *Science*, **2008**, *322*, 77–80; (c) Theriot, J. C.; Lim, C.-H.; Yang, H.; Ryan, M. D.; Musgrave, C. B.; Miyake, G. M. Organocatalyzed Atom Transfer Radical Polymerization Driven by Visible Light. *Science*, **2016**, *352*, 1082–1086; (d) Aycock, R. A.; Vogt, D. B.; Jui, N. T. A Practical and Scalable System for Heteroaryl Amino Acid Synthesis. *Chem. Sci.* **2017**, *8*, 7998–8003. Unactivated alkyl and aryl bromides can be the carbon radical sources using atom-transfer or transition-metal involved mechanism: (e) Devery, III, J. J. D.; Nguyen, J. D.; Dai, C.; Stephenson, C. R. J. Light-Mediated Reductive Debromination of Unactivated Alkyl and Aryl Bromides. *ACS Catal*. **2016**, *6*, 5962–5967; (f) Revol, G.; McCallum, T.; Morin, M.; Gagosz, F.; Barriault, L. Photoredox Transformations with Dimeric Gold Complexes. *Angew. Chem. Int. Ed*. **2013**, *52*, 13342–13345.

[7] Other types of photochemical reactions using aryl chlorides. Strong base-mediated reactions: (a) Budén, M. E.; Guastavino, J. F.; Rossi, R. A. Room-Temperature Photoinduced Direct C-H-Arylation via Base-Promoted Homolytic Aromatic Substitution. *Org. Lett*. **2013**, *15*, 1174–1177; (b) Cheng, Y.; Gu, X.; Li, P. Visible-Light Photoredox in Homolytic Aromatic Substitution: Direct Arylation of Arenes with Aryl Halides. *Org. Lett*. **2013**, *15*, 2664–2667; homolytic cleavage of C–Cl bonds: (c) Mfuh, A. M.; Doyle, J. D.; Chhetri, B.; Arman, H. D.; Larionov, O. V. Scalable, Metal- and Additive-Free, Photoinduced Borylation of Haloarenes and Quaternary Arylammonium Salts. *J. Am. Chem. Soc*. **2016**, *138*, 2985–2988; (d) Mfuh, A. M.; Nguyen, V. T.; Chhetri, B.; Burch, J. E.; Doyle, J. D.; Nesterov, V. N.; Arman, H. D.; Larionov, O. V. Additive- and Metal-Free, Predictably 1,2- and 1,3-Regioselective, Photoinduced Dual C-H/C-X Borylation of Haloarenes. *J. Am. Chem. Soc*. **2016**, *138*, 8408–8411. Reactions in which aryl radicals are not generated: (e) Jian, M.; Li, H.; Yang, H.; Fu, H. Room-Temperature Arylation of Thiols: Breakthrough with Aryl Chlorides. *Angew. Chem. Int. Ed*. **2017**, *56*, 874–879; (f) Shields, B. J.; Doyle, A. G. Direct C(sp3)-H Cross Coupling Enabled by Catalytic Generation of

Chlorine Radicals. *J. Am. Chem. Soc.* **2016**, *138*, 12719–12722; (g) Shaw, M. H.; Shurtleff, V. W.; Terrett, J. A.; Cuthbertson, J. D.; MacMillan, D. W. C. Native Functionality in Triple Catalytic Cross-Coupling: Sp3 C-H Bonds as Latent Nucleophiles. *Science*, **2016**, *352*, 1304–1308. A non-catalytic system: (h) Hasegawa, E.; Izumiya, N.; Fukuda, T.; Nemoto, K.; Iwamoto, H.; Takizawa, S.; Murata, S. Visible Light-Promoted Reductive Transformations of Various Organic Substances by using Hydroxyaryl-Substituted Benzimidazolines and Bases. *Tetrahedron* **2016**, *72*, 7805–7812.

[8] Several groups reported successful photochemical generation for aryl radicals from *activated* aryl chlorides: (a) Ghosh, I.; Shaikh, R. S.; König B. Sensitization-Initiated Electron Transfer for Photoredox Catalysis. *Angew. Chem. Int. Ed*. **2017**, *56*, 8544–8549; (b) Ghosh, I.; Ghosh, T.; Bardagi, J. I.; König, B. Reduction of Aryl Halides by Consecutive Visible Light-Induced Electron Transfer Processes. *Science* **2014**, *346*, 725–728; (c) Discekici, E. H.; Treat, N. J.; Poelma, S. O.; Mattson, K. M.; Hudson, Z. M.; Luo, Y.; Hawker, C. J.; de Alaniz, J. R. Metal-Free Photoredox Catalyst: Design and Application in Radical Dehalogenations. *Chem. Commun*. **2015**, *51*, 11705–11708.

[9] Yin, H.; Hertzog, J. E.; Mullane, K. C.; Carroll, P. J.; Manor, B. C.; Anna, J. M.; Schelter, E. J. The Hexachlorocerate(III) Anion: A Potent, Benchtop Stable, and Readily Available Ultraviolet a Photosensitizer for Aryl Chlorides. *J. Am. Chem. Soc*. **2016**, *138*, 16266–16273.

[10] Matsubara, R.; Shimada, T.; Kobori, Y.; Yabuta, T.; Osakai, T.; Hayashi, M. Photoinduced Charge-Transfer State of 4-Carbazolyl-3-(trifluoromethyl)benzoic Acid: Photophysical Property and Application to Reduction of Carbon-Halogen Bonds as a Sensitizer. *Chem. Asian J*. **2016**, *11*, 2006–2010.

[11] $E_{ox}^* = E_{ox} - E_{ex} + \omega$, where E_{ox}^* is the excited-state oxidation potential, E_{ox} the ground-state oxidation potential, E_{ex} the excitation energy, and ω is the work function. See Rehm, D.; Weller, A. Kinetics of Fluorescence Quenching by Electron and Hydrogen-Atom Transfer. *Isr. J. Chem*. **1970**, *8*, 259–271.

[12] CT-type photoredox catalysts show higher catalytic activity: Sartor, S. M.; McCarthy, B. G.; Pearson, R. M.; Miyake, G. M.; Damrauer, N. H. Exploiting Charge-Transfer States for Maximizing Intersystem Crossing Yields in Organic Photoredox Catalysts. *J. Am. Chem. Soc*. **2018**, *140*, 4778–4781.

[13] Shen, B.; Bedore, M. W.; Sniady, A.; Jamison, T. F. Continuous Flow Photo-Catalysis Enhanced using an Aluminum Mirror: Rapid and Selective Synthesis of 2'-Deoxy- and 2',3'- Dideoxynucleosides *Chem. Commun.* **2012**, *48*, 7444–7446.

[14] Saito, I.; Ikehira, H.; Kasatani, R.; Watanabe, M.; Matsuura, T. Photoinduced Reactions. 167. Selective Deoxygenation of Secondary alcohols by Photosensitized Electron-Transfer Reaction. A General Procedure for Deoxygenation of Ribonucleosides. *J. Am. Chem. Soc.* **1986**, *108*, 3115–3117.

[15] The accuracy of DFT calculations for CT states had been discussed. TD-DFT methods tend to overestimate transition energies. (a) Dreuw, A.; Head-Gordon, M. Failure of Time-Dependent Density Functional Theory for Long-Range Charge-Transfer Excited States: The Zincbacteriochlorin-Bacteriochlorin and Bacteriochlorophyll-Spheroidene Complexes. *J. Am. Chem. Soc.* **2004**, *126*, 4007–4016; (b) Jacquemin, D.; Wathelete, V.; Perpète, E. A.; Adamo, C. Extensive TD-DFT Benchmark: Singlet-Excited States of Organic Molecules. *J. Chem. Theory Comput*. **2009**, *5*, 2420–2435.

[16] (a) Mataga, N.; Kaifu, Y.; Koizumi, M. Solvent Effects upon Fluorescence Spectra and the Dipole Moments of Excited Molecules. *Bull. Chem. Soc. Jpn.* **1956**, *29*, 465; (b) Lippert, E. *Z.* Spectroscopic Determination of the Dipole Moment of Aromatic Compounds in the First Excited Singlet State. *Elektrochem.* **1957**, *61*, 962.

[17] The calculated S_1 state shows that both dimethylamino groups are almost co-planar to the carbazole plane, suggesting that the excited state of **CAR1** is of mesomeric intramolecular CT (MICT) character rather than intramolecular twisted CT (TICT). Dekhtyar, M.; Rettig, W.; Weigel, W. Mesomeric and Twisted Intramolecular-Charge-Transfer States as a Key to Polarity-Dependent Fluorescence of Donor-Acceptor-Substituted Aryl Pyrenes *Chem. Phys*. **2008**, *344*, 237–250.

[18] Moderate yields were due to the consumption of aryl radicals by a competitive hydrogen abstraction (41% and 27% yields of the reduced products were accompanied with **8m** and **8n**, respectively). A hydrogen atom probably comes from benzene Ar–H and the substrate's benzylic methylene. Li reported that the reaction of chlorobenzene with benzene gave biphenyl in 35% yield (Figure 1B, ref 7b). Note that in their case hydrogen atom abstraction from benzene by the phenyl radical does not lead to the loss of reactive species (the output is the identical phenyl radical), and they reported this reaction as a sole example using an aryl chloride as a substrate.

[19] The observation that reaction proceeds only upon constant irradiation does not decisively rule out the possibility of radical-chain process. Cismesia, M. A.; Yoon, T. P. Characterizing Chain Processes in Visible Light Photoredox Catalysis. *Chem. Sci*. **2015**, *6*, 5426–5434.

[20] For the demanding substrates such as unactivated aryl chlorides, judging from the Stern-Volmer plot that shows slow electron transfer from **CAR1***, the electron transfer from the triplet excited **CAR1** cannot be ruled out.

[21] The redox potential of $\mathbf{9}^{+}/\mathbf{9}$ or $\mathbf{11}^{+}/\mathbf{11}$ couples could not be found in the literature. Based on the redox potentials of similar stabilized carbon radicals, these redox potentials can be estimated to lie within a range of +1.0 and –1.0 V, which is much higher than those of aryl chlorides. Wayner, D. D. M.; McPhee, D. J.; Griller, D. Oxidation and Reduction Potentials of Transient Free Radicals. *J. Am. Chem. Soc.* **1988**, *110*, 132–137.

[22] In contrast, reactions based on the oxidation of demanding substrates have been increasingly studied. Selected examples: (a) Ohkubo, K.; Mizushima, K.; Iwata, R.; Fukuzumi, S. Selective Photocatalytic Aerobic Bromination with Hydrogen Bromide via an Electron-Transfer State of 9-Mesityl-10-methylacridinium ion. *Chem. Sci*. **2011**, *2*, 715–722; (b) Ohkubo, K.; Kobayashi, T.; Fukuzumi, S. Direct Oxygenation of Benzene to Phenol using Quinolinium Ions as Homogeneous Photocatalysts. *Angew. Chem. Int. Ed*. **2011**, *50*, 8652–8655; (c) Ohkubo, K.; Fujimoto, A.; Fukuzumi, S. Visible-Light-Induced Oxygenation of Benzene by the Triplet Excited State of 2,3-Dichloro-5,6-Dicyano-p-benzoquinone. *J. Am. Chem. Soc*. **2013**, *135*, 5368–5371; (d) Margrey, K. A.; McManus, J. B.; Bonazzi, S.; Zecri, F.; Nicewicz, D. A. Predictive Model for Site-Selective Aryl and Heteroaryl C-H Functionalization via Organic Photoredox Catalysis. *J. Am. Chem. Soc*. **2017**, *139*, 11288–11299; (e) Pitzer, L.; Sandfort, F.; Strieth-Kalthoff, F.; Glorius, F. Intermolecular Radical Addition to Carbonyls Enabled by Visible Light Photoredox Initiated Hole Catalysis. *J. Am. Chem. Soc.* **2017**, *139*, 13652–13655; (f) Margrey, K. A.; Levens, A.; Nicewicz, D. A. Direct Aryl C-H Amination with Primary Amines using Organic Photoredox Catalysis. *Angew. Chem. Int. Ed*. **2017**, *56*, 15644–15648; (g) Niu, L.; Yi, H.; Wang, S.; Liu, T.; Liu, J.; Lei, A. Photo-Induced Oxidant-Free ocidative C-H/N-H Cross-Coupling between Arenes and Azoles. *Nature Commun*. **2017**, *8*, 14226.

[23] Shen, B.; Jamison, F. T. Continuous Flow Photochemistry for the Rapid and Selective Synthesis of 2'-Deoxy and 2',3'-Dideoxynucleosides. *Aust. J. Chem.* **2013**, *66*, 157–164.

[24] Yus, M.; Ortiz, R.; Huerta, F. F. Intramolecular Carbolithiation Promoted by a DTBB-Catalyzed Chlorine-lithium Exchange. *Tetrahedron* **2003**. *59*, 8525–8542.

[25] Gaussian 09, R. D., Frisch, M. J.; Trucks, G. W.; Schlegel, H. B.; Scuseria, G. E.; Robb, M. A.; Cheeseman, J. R.; Scalmani, G.; Barone, V.; Mennucci, B.; Petersson, G. A.; Nakatsuji, H.; Caricato, M.; Li, X.; Hratchian, H. P.; Izmaylov, A. F.; Bloino, J.; Zheng, G.;

Sonnenberg, J. L.; Hada, M.; Ehara, M.; Toyota, K.; Fukuda, R.; Hasegawa, J.; Ishida, M.; Nakajima, T.; Honda, Y.; Kitao, O.; Nakai, H.; Vreven, T.; Montgomery, J. A., Jr.; Peralta, J. E.; Ogliaro, F.; Bearpark, M.; Heyd, J. J.; Brothers, E.; Kudin, K. N.; Staroverov, V. N.; Kobayashi, R.; Normand, J.; Raghavachari, K.; Rendell, A.; Burant, J. C.; Iyengar, S. S.; Tomasi, J.; Cossi, M.; Rega, N.; Millam, J. M.; Klene, M.; Knox, J. E.; Cross, J. B.; Bakken, V.; Adamo, C.; Jaramillo, J.; Gomperts, R.; Stratmann, R. E.; Yazyev, O.; Austin, A. J.; Cammi, R.; Pomelli, C.; Ochterski, J. W.; Martin, R. L.; Morokuma, K.; Zakrzewski, V. G.; Voth, G. A.; Salvador, P.; Dannenberg, J. J.; Dapprich, S.; Daniels, A. D.; Farkas, Ö.; Foresman, J. B.; Ortiz, J. V.; Cioslowski, J.; Fox, D. J. Gaussian, Inc., Wallingford CT, 2009.

[26] (a) Elvington, M. C.; Brewer, K. J. Electrochemistry In *Application of Physical Methods to Inorganic and Bioinorganic Chemistry*; Scott, R. A.; Lukehart, C. M., Eds.; Wiley: Chichester, 2007; pp 17–38; (b) Gennett, T.; Milner, D. F.; Weaver, M. J. *J. Phys. Chem.* Role of Solvent Reorganization Dynamics in Electron-Transfer Processes. Theory-Experiment Comparisons for Electrochemical and Homogeneous Electron Exchange Involving Metallocene Redox Couples. **1985**, *89*, 2787–2794.

[27] Pan, X.; Lacôte, E.; Lalevée, J.; Curran, D. P. Polarity Reversal Catalysis in Radical Reductions of Halides by N-Heterocyclic Carbene Boranes. *J. Am. Chem. Soc.* **2012**, *134*, 5669–5674.

[28] Liu, Y. X.; Xue, D.; Wang, J. D.; Zhao, C. J.; Zou, Q. Z.; Wang, C.; Xiao, J. Room-Temperature Arylation of Arenes and Heteroarenes with Diaryl-iodonium Salts by Photoredox Catalysis. *Synlett* **2013**, *24*, 507–513.

[29] Trofimov, B. A.; Mikhaleva, A. I.; Ivanov, A. V.; Shcherbakova, V. S. Expedient One-pot Synthesis of Pyrroles from Ketones, Hydroxylamine, and 1,2-Dichloroethane. *Tetrahedron* **2015**, *71*, 124–128.

[30] Nadres, T. E.; Lazareva, A.; Daugulis, O. Palladium-Catalyzed Indole, Pyrrole, and Furan Arylation by Aryl Chlorides. *J. Org. Chem.* **2011**, *76*, 471–483.

[31] Ghosh, I.; König, B. Chromoselective Photocatalysis: Controlled Bond Activation through Light-Color Regulation of Redox Potentials. *Angew. Chem. Int. Ed.* **2016,** *55*, 7676–7679.

[32] Hofmann, J.; Gans, E.; Clark, T.; Heinrich, M. R. Radical Arylation of Anilines and Pyrroles via Aryldiazotates. *Chem. Eur. J.* **2017**, *23*, 9647–9656.

[33] Kocaoglu, E.; Karaman, A. M.; Tokgöz, H.; Talaz, O. Transition-Metal Catalyst Free Oxidative Radical Arylation of N-Methylpyrrole. *ACS Omega* **2017**, *2*, 5000–5004.

[34] Agata, R.; Iwamoto, T.; Nakagawa, N.; Isozaki, K.; Hatakeyama, T.; Takaya, H.; Nakamura, M. Iron Fluoride/N-Heterocyclic Carbene Catalyzed Cross Coupling between Deactivated Aryl Chlorides and Alkyl Grignard Reagents with or without β-Hydrogens. *Synthesis* **2015**, *47*, 1733–1740.

Insert Table of Contents artwork here